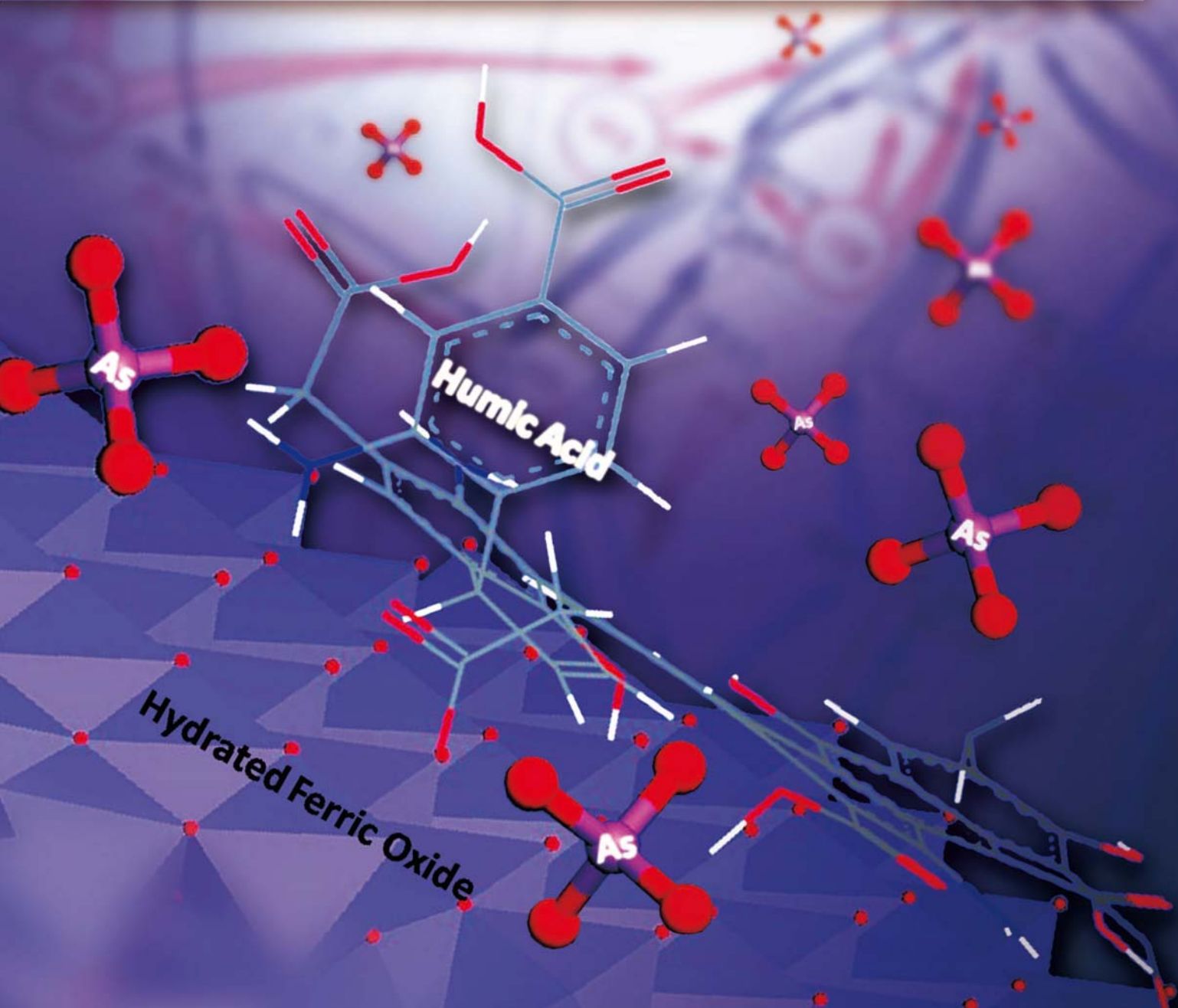


# JES

JOURNAL OF  
ENVIRONMENTAL  
SCIENCES

ISSN 1001-0742  
CN 11-2629/X

February 1, 2014 Volume 26 Number 2  
[www.jesc.ac.cn](http://www.jesc.ac.cn)



Sponsored by  
Research Center for Eco-Environmental Sciences  
Chinese Academy of Sciences

## CONTENTS

## Aquatic environment

Removal of total cyanide in coking wastewater during a coagulation process: Significance of organic polymers Jian Shen, He Zhao, Hongbin Cao, Yi Zhang, Yongsheng Chen .....	231
Removal of arsenate with hydrous ferric oxide coprecipitation: Effect of humic acid Jingjing Du, Chuanyong Jing, Jinming Duan, Yongli Zhang, Shan Hu .....	240
Arsenic removal from groundwater by acclimated sludge under autohydrogenotrophic conditions Siqing Xia, Shuang Shen, Xiaoyin Xu, Jun Liang, Lijie Zhou .....	248
Characteristics of greenhouse gas emission in three full-scale wastewater treatment processes Xu Yan, Lin Li, Junxin Liu .....	256
Effect of temperature on anoxic metabolism of nitrites to nitrous oxide by polyphosphate accumulating organisms Zhijia Miao, Wei Zeng, Shuying Wang, Yongzhen Peng, Guihua Cao, Dongchen Weng, Guisong Xue, Qing Yang .....	264
Efficacy of two chemical coagulants and three different filtration media on removal of <i>Aspergillus flavus</i> from surface water Hamid Mohammad Al-Gabr, Tianling Zheng, Xin Yu .....	274
Beyond hypoxia: Occurrence and characteristics of black blooms due to the decomposition of the submerged plant <i>Potamogeton crispus</i> in a shallow lake Qiushi Shen, Qilin Zhou, Jingge Shang, Shiguang Shao, Lei Zhang, Chengxin Fan .....	281
Spatial and temporal variations of two cyanobacteria in the mesotrophic Miyun reservoir, China Ming Su, Jianwei Yu, Shenling Pan, Wei An, Min Yang .....	289
Quantification of viable bacteria in wastewater treatment plants by using propidium monoazide combined with quantitative PCR (PMA-qPCR) Dan Li, Tiezheng Tong, Siyu Zeng, Yiwen Lin, Shuxu Wu, Miao He .....	299
Antimony(V) removal from water by hydrated ferric oxides supported by calcite sand and polymeric anion exchanger Yangyang Miao, Feichao Han, Bingcai Pan, Yingjie Niu, Guangze Nie, Lu Lv .....	307
A comparison on the phytoremediation ability of triazophos by different macrophytes Zhu Li, Huiping Xiao, Shuiping Cheng, Liping Zhang, Xiaolong Xie, Zhenbin Wu .....	315
Biostability in distribution systems in one city in southern China: Characteristics, modeling and control strategy Pinpin Lu, Xiaojian Zhang, Chiqian Zhang, Zhangbin Niu, Shuguang Xie, Chao Chen .....	323

## Atmospheric environment

Characteristics of ozone and ozone precursors (VOCs and NO <sub>x</sub> ) around a petroleum refinery in Beijing, China Wei Wei, Shuiyuan Cheng, Guohao Li, Gang Wang, Haiyang Wang .....	332
Identification of sources of lead in the atmosphere by chemical speciation using X-ray absorption near-edge structure (XANES) spectroscopy Kohei Sakata, Aya Sakaguchi, Masaharu Tanimizu, Yuichi Takaku, Yuka Yokoyama, Yoshio Takahashi .....	343
Online monitoring of water-soluble ionic composition of PM <sub>10</sub> during early summer over Lanzhou City Jin Fan, Xiaoying Yue, Yi Jing, Qiang Chen, Shigong Wang .....	353
Effect of traffic restriction on atmospheric particle concentrations and their size distributions in urban Lanzhou, Northwestern China Suping Zhao, Ye Yu, Na Liu, Jianjun He, Jinbei Chen .....	362

## Environmental health and toxicology

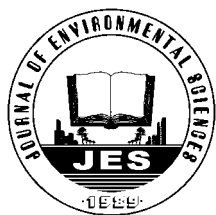
A review on completing arsenic biogeochemical cycle: Microbial volatilization of arsines in environment Peipei Wang, Guoxin Sun, Yan Jia, Andrew A Meharg, Yongguan Zhu .....	371
Alginate modifies the physiological impact of CeO <sub>2</sub> nanoparticles in corn seedlings cultivated in soil Lijuan Zhao, Jose R. Peralta-Videa, Bo Peng, Susmita Bandyopadhyay, Baltazar Corral-Diaz, Pedro Osuna-Avila, Milka O. Montes, Arturo A. Keller, Jorge L. Gardea-Torresdey .....	382
Humification characterization of biochar and its potential as a composting amendment Jining Zhang, Fan Lü, Chenghao Luo, Liming Shao, Pinjing He .....	390
Immigrant <i>Pantoea agglomerans</i> embedded within indigenous microbial aggregates: A novel spatial distribution of epiphytic bacteria Qing Yu, Anzhou Ma, Mengmeng Cui, Xuliang Zhuang, Guoqiang Zhuang .....	398
Remediation of nutrient-rich waters using the terrestrial plant, <i>Pandanus amaryllifolius</i> Roxb. Han Ping, Prakash Kumar, Bee-Lian Ong .....	404

---

Construction of a dual fluorescence whole-cell biosensor to detect <i>N</i> -acyl homoserine lactones	
Xuemei Deng, Guoqiang Zhuang, Anzhou Ma, Qing Yu, Xuliang Zhuang	415
Digestion performance and microbial community in full-scale methane fermentation of stillage from sweet potato-shochu production	
Tsutomu Kobayashi, Yueqin Tang, Toyoshi Urakami, Shigeru Morimura, Kenji Kida	423
Health risk assessment of dietary exposure to polycyclic aromatic hydrocarbons in Taiyuan, China	
Jing Nie, Jing Shi, Xiaoli Duan, Beibei Wang, Nan Huang, Xiuge Zhao	432
Acute toxicity formation potential of benzophenone-type UV filters in chlorination disinfection process	
Qi Liu, Zhenbin Chen, Dongbin Wei, Yuguo Du	440
Exposure measurement, risk assessment and source identification for exposure of traffic assistants to particle-bound PAHs in Tianjin, China	
Xiaodan Xue, Yan You, Jianhui Wu, Bin Han, Zhipeng Bai, Naijun Tang, Liwen Zhang	448

## Environmental catalysis and materials

Fabrication of Bi <sub>2</sub> O <sub>3</sub> /TiO <sub>2</sub> nanocomposites and their applications to the degradation of pollutants in air and water under visible-light	
Ashok Kumar Chakraborty, Md Emran Hossain, Md Masudur Rhaman, K M A Sobahan	458
Comparison of quartz sand, anthracite, shale and biological ceramsite for adsorptive removal of phosphorus from aqueous solution	
Cheng Jiang, Liyue Jia, Bo Zhang, Yiliang He, George Kirumba	466
Catalytic bubble-free hydrogenation reduction of azo dye by porous membranes loaded with palladium nanoparticles	
Zhiqian Jia, Huijie Sun, Zhenxia Du, Zhigang Lei	478
Debromination of decabromodiphenyl ether by organo-montmorillonite-supported nanoscale zero-valent iron:	
Preparation, characterization and influence factors	
Zhihua Pang, Mengyue Yan, Xiaoshan Jia, Zhenxing Wang, Jianyu Chen	483
Serial parameter: CN 11-2629/X*1989*m*261*en*P*30*2014-2	

Available online at [www.sciencedirect.com](http://www.sciencedirect.com)

Journal of Environmental Sciences

[www.jesc.ac.cn](http://www.jesc.ac.cn)

## Identification of sources of lead in the atmosphere by chemical speciation using X-ray absorption near-edge structure (XANES) spectroscopy

Kohei Sakata<sup>1,\*</sup>, Aya Sakaguchi<sup>1</sup>, Masaharu Tanimizu<sup>1,2</sup>, Yuichi Takaku<sup>3</sup>, Yuka Yokoyama<sup>1</sup>, Yoshio Takahashi<sup>1,2</sup>

<sup>1</sup>. Department of Earth and Planetary Systems Science, Hiroshima University, Higashi-Hiroshima, Hiroshima 739-8526, Japan

<sup>2</sup>. Kochi Institute for Core Sample Research, Japan Agency for Marine-Earth Science and Technology, Monobe-Otsu 200, Nankoku, Kochi 783-8502, Japan

<sup>3</sup>. Institute for Environmental Sciences, Rokkasho, Aomori 039-3212, Japan

### ARTICLE INFO

#### Article history:

Received 19 February 2013

revised 17 July 2013

accepted 28 July 2013

#### Keywords:

lead

lead speciation

XAFS spectroscopy

size-fractionated aerosol sample

DOI: 10.1016/S1001-0742(13)60430-1

### ABSTRACT

Sources of Pb pollution in the local atmosphere together with Pb species, major ions, and heavy metal concentrations in a size-fractionated aerosol sample from Higashi-Hiroshima (Japan) have been determined by X-ray absorption near-edge structure (XANES) spectroscopy, ion chromatography, and ICP-MS/AES, respectively. About 80% of total Pb was concentrated in fine aerosol particles. Lead species in the coarse aerosol particles were  $\text{PbC}_2\text{O}_4$ ,  $2\text{PbCO}_3 \cdot \text{Pb}(\text{OH})_2$ , and  $\text{Pb}(\text{NO}_3)_2$ , whereas Pb species in the fine aerosol particles were  $\text{PbC}_2\text{O}_4$ ,  $\text{PbSO}_4$ , and  $\text{Pb}(\text{NO}_3)_2$ . Chemical speciation and abundance data suggested that the source of Pb in the fine aerosol particles was different from that of the coarse ones. The dominant sources of Pb in the fine aerosol particles were judged to be fly ash from a municipal solid waste incinerator and heavy oil combustion. For the coarse aerosol particles, road dust was considered to be the main Pb source. In addition to Pb species, elemental concentrations in the aerosols were also determined. The results suggested that Pb species in size-fractionated aerosols can be used to identify the origin of aerosol particles in the atmosphere as an alternative to Pb isotope ratio measurement.

## Introduction

Lead (Pb) is one of the most prominent pollutants, especially for atmospheric pollution, as a result of extensive use of leaded gasoline throughout the world (e.g. Nriagu, 1990; Mukai et al., 1993; Chen et al., 2005). In recent years, atmospheric Pb concentrations have dramatically decreased due to the use of lead-free gasoline. However, atmospheric pollution by Pb is still recognized as a potential health problem (Murphy et al., 2007). Moreover transboundary air-pollution is also a key topic from an international relations perspective. Thus, there is an ongoing need to

monitor the concentrations, species, and sources of Pb in the atmosphere.

The measurement of Pb isotope ratios has long been employed as a powerful tool to identify the sources of Pb pollution (e.g. Rabinowitz and Wetherill, 1972; Mukai et al., 1993; Sakata et al., 2000). Furthermore, such ratios can be a good tracer for air-mass transportation because Pb isotope ratios differ significantly depending on the emission area/source (e.g. Maring et al., 1987; Mukai et al., 1994; Bollhöfer and Rosman, 2000, 2001; Shimamura et al., 2007; Inoue and Tanimizu, 2008). Following the usage restriction of leaded gasoline, however, Pb isotope ratio measurements may not be used for source identification and as an air-mass tracer in recent years, because the Pb isotope ratio has not been well characterized according to

\* Corresponding author. E-mail: kou-sakata@hiroshima-u.ac.jp

each source (Mizoguchi et al., 2012).

Lineage analysis and principal component analysis of major and minor elemental components in aerosols have been used to identify sources of Pb in the atmosphere (Salma et al., 2002; Wang et al., 2006). X-ray diffraction (XRD) measurements have also been conducted for speciation analysis of Pb in the atmosphere (Biggins and Harrison, 1979; Sturges and Harrison, 1989). Statistical methods, based on elemental composition data, which are indirect methods, lack the specificity for unambiguous identification of Pb species in the atmosphere. Also in the case of XRD measurements, since Pb is a minor component in the aerosol particles examined, specific Pb species have not been identified. As an alternative direct method for Pb speciation, scanning electron microscopy with energy dispersive X-ray spectroscopy (SEM-EDS/EDX) has been employed to determine the elemental compositions of single aerosol particles (e.g. Linton et al., 1980; Moffet et al., 2008). However, it is not easy to estimate the average composition of various Pb species in an aerosol sample by such particle analysis.

As a powerful tool to determine chemical species of heavy metals directly in aerosols, X-ray absorption fine structure (XAFS) spectroscopy can be proposed. With XAFS spectroscopy, there is almost no spectral interferences from co-existing elements, that is, each element exhibits a characteristic and unique X-ray absorption edge. Furthermore, information on the chemical form of the heavy metals in the aerosol can be obtained with minimal/no sample pretreatment, even if the concentration of the element in the sample is low (e.g. a few tens of ppm). Actually, many studies on chemical speciation of heavy metals in environmental materials, including aerosols by XAFS spectroscopy, have been reported in recent years (e.g. Manceau et al., 1996; Takahashi et al., 2006; Higashi and Takahashi, 2009). However, there are few studies on the determination of Pb species in aerosols by XAFS spectroscopy. Tan et al. (2006) reported that the Pb species in PM<sub>10</sub> and PM<sub>2.5</sub> aerosols in Shanghai, China were PbO, PbCl<sub>2</sub>, and PbSO<sub>4</sub> by analyzing Pb L<sub>III</sub>-edge absorption with the Si(111) monochromator. They concluded that the dominant source of these Pb species were from coal combustion. On the other hand, Pb species in total suspended particles (TSP), collected along a busy road in the city center of Osaka, Japan were PbS, PbCO<sub>3</sub>, PbSO<sub>4</sub>, and/or PbCl<sub>2</sub> following Pb L<sub>III</sub>-edge absorption measurements using the Si(111) monochromator (Funasaka et al., 2008). These results showed that Pb species in atmospheric aerosols might consist of different forms depending on the location, which, in turn, might reflect differences in chemical processing and sources of Pb. However, it is difficult to distinguish Pb species using L<sub>III</sub>-edge X-ray adsorption near-edge structure (XANES) spectra. This is because the spectra from some species are very similar without distinctive features. In this study,

we have employed a double-crystal of Si(311) for measurement of Pb L<sub>III</sub>-edge absorption of aerosol samples to obtain better energy resolution than that afforded by the Si(111) crystal as used in previous studies (Tan et al., 2006; Funasaka et al., 2008). It was anticipated that the improved spectral resolution would permit the differentiation of Pb species in the aerosol samples.

It is well known that the formation mechanisms of fine and coarse aerosol particles are distinctly different. Coarse aerosol particles (> 2.1 μm) typically originate from wind-blown particles such as sea spray and soil, whereas fine aerosol particles (< 2.1 μm) originate from condensation and/or coagulation of precursor gases related to high temperature combustion processes (Jacob, 1999). This suggests that the chemical species of heavy metals in aerosol particles of differing particle size may be different due to differences of source and/or particle formation mechanisms. That is, the chemical species and concentration distribution of heavy metals in the various aerosol particles will be constrained by the formation mechanisms of the particles. Furthermore, the toxicity and health effects of heavy metals can be very different depending on the chemical species and aerosol size. Thus, it is important to clarify information on chemical species and concentration distribution in each aerosol size to evaluate the potential effect on human health. Hence, size distribution analysis for chemical species of heavy metals in aerosols including concentrations will contribute not only to the development of new problem-solving approaches in atmospheric pollution but also to advancing knowledge in atmospheric chemistry. To date then, the chemical species of heavy metals and formation mechanisms of the species in aerosol samples have yet to be clarified.

In this research, we have collected 6 size-fractionated aerosol samples for the study of Pb species and major and trace elemental composition. A key feature of our approach is the use of a double-crystal of Si(311), which provides high resolution monochromatic incident X-ray for measurement of Pb L<sub>III</sub>-edge XANES of aerosol samples. The improved energy resolution is expected to permit the differentiation of Pb species in aerosol samples of different origins. To confirm the accuracy of the combination of Pb species in each size fractionated single particle, micro(μ)-XRF-XAFS analysis was conducted. In addition, accuracy of speciation by XAFS can be improved if the number of end members assumed in the fitting of the spectra is reduced. In this regard, size-fractionated sampling also contributes to an improved reliance of XAFS analysis, since it is expected that Pb species are different among the different particle sizes.

If the Pb species and the associated formation mechanisms in size-fractionated aerosol samples can be clarified for samples from a single sampling site such as in Hiroshima, it may be possible for the methodology to be applied to other locations in the world. In addition to the six



aerosol samples analyzed, samples representing candidate atmospheric emission sources of Pb were also examined. This is the first such report on the determination and characterization of Pb species in size-fractionated aerosols and at high energy resolution with XAFS spectroscopy.

## 1 Methods

### 1.1 Sampling

Size-fractionated aerosol samples were collected on the roof of a building (10 m above ground level) at Higashi-Hiroshima City (34.40°N, 132.71°E; 9 to 23 October, 2012) (**Fig. 1**). We chose the autumn for the first step of this study, because October in Japan generally does not have any particular climatic events such as yellow sand and typhoon events. Thus, the result from this sample may be basic information that can be compared with those obtained in yellow sand and typhoon events. Aerosol samples were collected on a cellulose filter (TE-230WH, Tish Environmental, Inc., USA) for stages 1 to 5 and a Whatman 41 filter (8 × 10 inch, Whatman, USA) for stage-BF using a high-volume air sampler (MODEL-123SL, Kimoto, Japan) with cascade impactor (TE-236, Tisch Environmental Inc., USA). The flow rate was 0.566 m<sup>3</sup>/min and the total volume of air sampled was 11572.1 m<sup>3</sup>. The aerosol diameter of each stage is as follows: Stage 1: > 10.2 μm; stage-2: 10.2–4.2 μm; stage-3: 4.2–2.1 μm; stage-4: 2.1–1.3 μm;

stage-5: 1.3–0.69 μm; stage-BF: < 0.69 μm. Stages 1 to 3 collected coarse aerosol particles, whereas stages 4, 5, and the backup filter collected fine aerosol particles. Each cellulose filter was weighed before and after sampling and maintained under constant humidity (20%) in a desiccator, as described by Furukawa and Takahashi (2011).

Samples corresponding to local sources of Pb emissions, both anthropogenic and natural samples, were also collected. Two kinds of fly ash from a municipal solid waste incinerator (MSWI), which is located about 8 km from the sampling site for aerosol samples, were collected. One of these fly ashes was a dispersed material from a chimney and the other was a residual fly ash from an incinerator. The dispersed fly ash sample was collected by a high volume air sampler (HV-500F, Sibata, Japan) immediately at the exit of the chimney and residual ash was obtained by a spatula from the bottom of the chimney. A heavy oil combustion sample was also collected by the high volume air sampler (HV-500F, Sibata, Japan) immediately at the exit of the chimney. Actually, oil fired boilers and combustion equipment are operated in many public facilities and factories and these, currently, are important sources of Pb emissions in Japan (Sakata et al., 2000; Wang et al., 2005). TSP was also collected by the high volume air sampler (HV-500F, Sibata, Japan) at the Yasumiyama tunnel, Kure, Japan. Road dust on Route 2 in Hiroshima City and resuspended particles on a roof were collected by a spatula. Weathered Hiroshima granite, the main lithology of the area, was sampled as a possible natural Pb source. The grain size distribution of road dust, resuspended particles, and weathered Hiroshima granite showed a wide range of particle sizes (0.4–100 μm) and the average size (weight basis) was relatively large (greater than 50 μm).

### 1.2 XANES analysis

For identification of Pb species in samples, Pb L<sub>III</sub>-edge (13.041 keV) XANES spectra were recorded at SPring-8 beamline BL01B1 in Hyogo, Japan and on NW10A at the KEK Photon Factory Advanced Ring (PF-AR) in Tsukuba, Japan. The X-ray energy ranges for the Si(111) and Si(311) monochromators are about 5 to 30 keV and 10 to 40 keV, respectively. Therefore, XAFS experiments on Pb can be carried out by both the Si(111) and the Si(311) monochromator. We employed monochromatic radiation from a pair of Si(311) crystals, the energy resolution of which is higher than that of the Si(111) crystal used in previous studies (Tan et al., 2006; Funasaka et al., 2008). An energy resolution ( $\Delta E/E$ ) around 13 keV, with the Si(111) monochromator, which is the Pb L<sub>III</sub>-edge absorption energy, is about  $2 \times 10^{-4}$ , whereas  $\Delta E/E$  with the Si(311) monochromator is about  $3 \times 10^{-5}$ .

Measurement of all samples was carried out in fluorescence mode with a 19-element Ge solid state detector (SSD). The energy of the Pb L<sub>III</sub>-edge XANES was

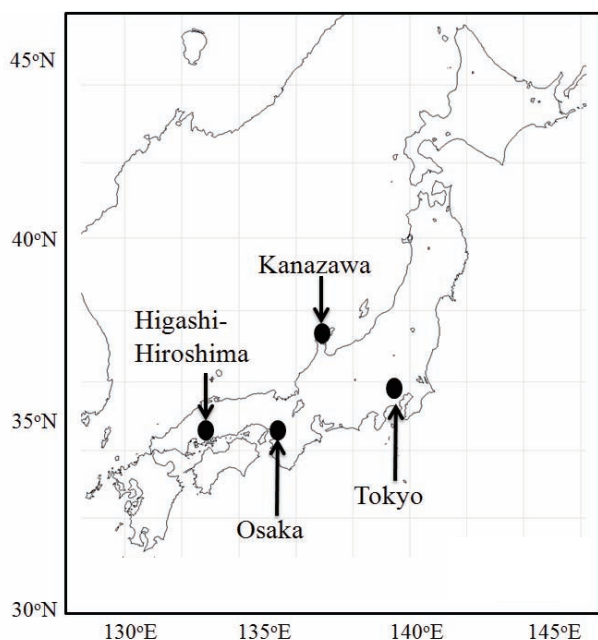


**Fig. 1** Sampling sites of size-fractionated aerosol sample and sources of emission (Higashi-Hiroshima) Kanazawa, Tokyo, and Osaka are comparative sites of Pb species and heavy metal concentrations in the atmosphere, Japan (Sakata et al., 2000; Wang et al., 2006; Funasaka et al., 2008).

calibrated with PbO, which yielded a definitive peak maximum (13.041 keV) for the XANES spectrum. For XANES measurements in aerosol samples with low Pb concentrations, each aerosol filter sample was cut into small size and 4–5 pieces from one filter were placed one on top of the other in order to increase the Pb signal intensity. One to four scans (from 12.920 to 13.280 keV) were summed in order to improve the signal to noise ratio. Repeat scans gave identical spectra, showing that photodegradation of Pb species could be neglected. Twelve different Pb compounds (PbO, PbS, PbSO<sub>4</sub>, PbCO<sub>3</sub>, Pb(NO<sub>3</sub>)<sub>2</sub>, PbCl<sub>2</sub>, PbCrO<sub>4</sub>, PbMoO<sub>4</sub>, PbC<sub>2</sub>O<sub>4</sub>, Pb(OH)<sub>2</sub>, 2PbCO<sub>3</sub>·Pb(OH)<sub>2</sub>, and Pb<sub>3</sub>(PO<sub>4</sub>)<sub>2</sub>) and Pb metal foil were analyzed as reference materials. Micro-XANES spectra at Pb L<sub>III</sub>-edge were collected for single particle of our aerosol samples at BL37XU in SPring-8, Japan (Terada et al., 2004) to confirm the results of the bulk XANES analyses. All details of  $\mu$ -XRF-XANES analyses for Pb in aerosol samples will be presented in Sakata et al., (in prep).

The linear combination fitting of XANES spectra for aerosol samples with standard materials was performed using REX 2000 software (Rigaku, Japan). To estimate the goodness-of-fit for the XANES spectra, the *R* value corresponding to the energy region for the fitting was employed. The *R* value is defined as:

$$R^2 = \frac{\sum (I_s(E) - I_{cal}(E))^2}{\sum I_{cal}(E)^2} \quad (1)$$

where,  $I_s$  and  $I_{cal}$  are the normalized absorptions of the samples and the calculated values, respectively. The energy range for fitting the Pb-L<sub>III</sub> edge XANES was from 12.990 to 13.110 keV.

The analyses for major and trace elemental composition in each size fraction are shown in Supplement materials.

## 2 Results and discussion

### 2.1 Lead species in atmosphere and possible Pb sources

Representative Pb-L<sub>III</sub> XANES spectra for fine and coarse aerosol particles and reference materials using a linear combination fitting of the samples are shown in Fig. 2. The combination of reference Pb species which had the smallest *R* value was used as the best fitting results. Figure 3 shows the XANES spectra of all reference materials. Generally, the Pb L<sub>III</sub>-edge XANES spectra of divalent Pb species are very similar and it is difficult to confirm the presence of Pb species in our samples given the low concentrations of Pb. However, we successfully obtained Pb L<sub>III</sub>-edge XANES spectra at high energy resolution using the Si(311) monochromator. As a result, XANES spectra of coarse and fine aerosol particles are clearly different. These results suggested that the dominant Pb

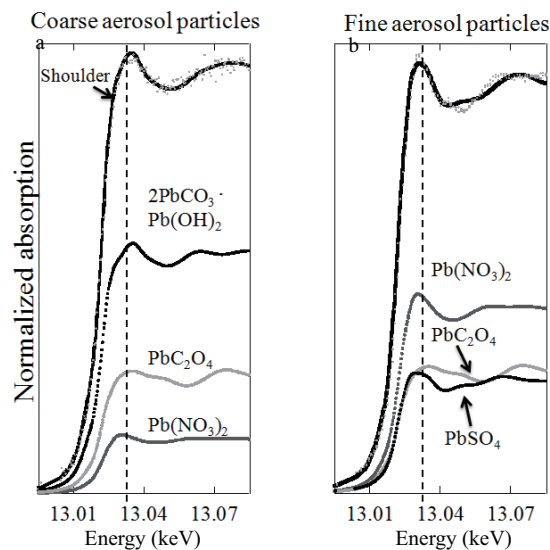


**Fig. 2** (a) Pb-L<sub>III</sub> XANES spectra for coarse (2.1–4.2  $\mu$ m) and reference materials using linear combination fitting. (b) Pb-L<sub>III</sub> XANES spectra for fine (0.69–1.3  $\mu$ m) and reference materials using linear combination fitting. Dashed line: main peak top position of aerosol sample. XANES spectrum of samples strongly reflect the most dominant Pb species. Peak top energy is slightly different between coarse and fine aerosol particles depending on the dominant Pb species.

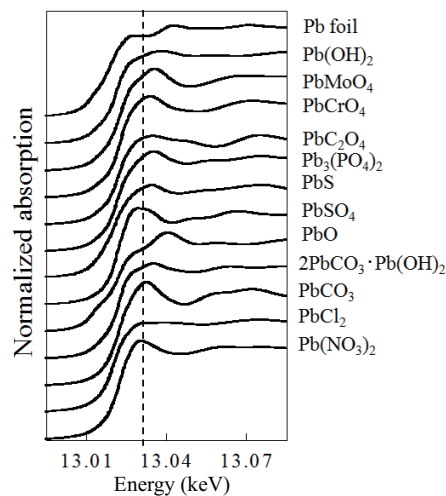


**Fig. 3** Pb-L<sub>III</sub> XANES spectra of reference materials. Pb(0) foil and twelve Pb(II) compounds served as reference materials. Dashed line is drawn at 13.03 keV. Peak tops for PbSO<sub>4</sub> and Pb(NO<sub>3</sub>)<sub>2</sub> are slightly lower than 13.03 keV, whereas that of PbO is slightly higher than 13.03 keV.

species in coarse and fine aerosol particles are different.

For the fitting of XANES spectra, analysis to identify Pb species was performed as follows: the spectra of coarse (2.1–4.2  $\mu$ m) aerosol particles have a very small shoulder at around 13.025 keV. The XANES spectra of PbO, PbMoO<sub>4</sub> and 2PbCO<sub>3</sub>·Pb(OH)<sub>2</sub> have a small shoulder around this energy and some of these species have a spectrum typical of coarse aerosol particles. The peak top of PbO is located at 13.04 keV, whereas those of

coarse aerosol particles,  $\text{PbMoO}_4$ , and  $2\text{PbCO}_3 \cdot \text{Pb(OH)}_2$  are at 13.03 keV. Therefore,  $\text{PbO}$  is not the dominant Pb species in this case. The XANES spectra of  $\text{PbMoO}_4$  and  $2\text{PbCO}_3 \cdot \text{Pb(OH)}_2$  are quite similar. The second peak top of  $\text{PbMoO}_4$  is slightly higher than that of  $2\text{PbCO}_3 \cdot \text{Pb(OH)}_2$ . However, this visual feature is not sufficient to identify the most dominant Pb species. Regarding the results of linear combination fitting using the spectra of these reference materials, the smallest  $R$  value for the combination of Pb species including  $\text{PbMoO}_4$  was estimated as 0.020. At the same time, the smallest  $R$  value including  $2\text{PbCO}_3 \cdot \text{Pb(OH)}_2$  was 0.014. The linear combination fitting which included both  $\text{PbMoO}_4$  and  $2\text{PbCO}_3 \cdot \text{Pb(OH)}_2$  gave a negative fitting value for  $\text{PbMoO}_4$ . This means that the combination of Pb species for linear combination fitting with  $\text{PbMoO}_4$  is not appropriate. Therefore, it can be concluded that the XANES spectra of coarse aerosol particles is a strong indicator of  $2\text{PbCO}_3 \cdot \text{Pb(OH)}_2$ .

In the case of XANES spectra for fine aerosol particles (0.69 to 1.3  $\mu\text{m}$ ), the first peak top is located at slightly below 13.03 keV. The XANES spectra of  $\text{PbSO}_4$  and  $\text{Pb(NO}_3)_2$  have distinct peaks: the first peak top is located at slightly below 13.03 keV (Fig. 3 dashed line at 13.03 keV). In the case of the other reference materials, the peak top for the first peak was at 13.03 to 13.04 keV. Small differences in the energy of the first peak top is very important to identify and distinguish  $\text{PbSO}_4$  and  $\text{Pb(NO}_3)_2$ . Therefore, it can be said that fine aerosol particles clearly contain  $\text{PbSO}_4$  and  $\text{Pb(NO}_3)_2$ .

Figure 4 (gray circles plot) shows the Pb-L<sub>III</sub> XANES spectra for all samples of coarse and fine aerosol particles investigated. The solid lines in the figure are the results of the linear combination fitting of the sample spectrum with reference samples. All aerosol samples and candidate Pb source materials could be measured and the spectra for the aerosol samples fitted well with reference samples.

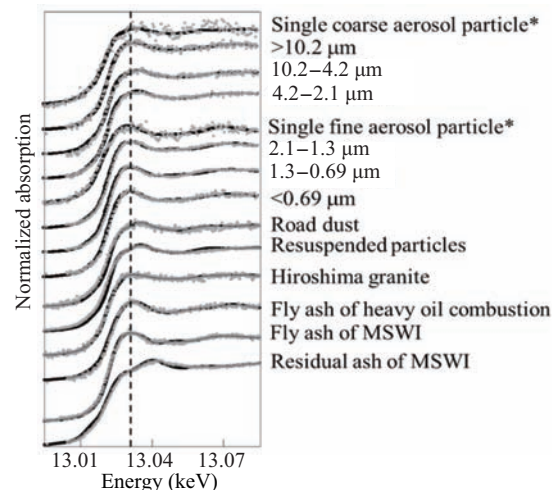


Fig. 4 Pb-L<sub>III</sub> XANES spectra of coarse and fine aerosol particles, selected samples and reference materials using linear combination fitting. Gray circles are normalized spectra and black solid line is fitted spectra. \*: example of spectrum of m-XANES analysis for single aerosol particles from size-fractionated aerosol samples.

The fitting results in Fig. 4 are shown in Table 1 as relative ratios of Pb species (%) together with  $R$  values for each sample. The lead species in the size ranges >10.2  $\mu\text{m}$ , 10.2–4.2 and 4.2–2.1  $\mu\text{m}$  are coarse aerosol particles and are  $\text{PbC}_2\text{O}_4$ ,  $2\text{PbCO}_3 \cdot \text{Pb(OH)}_2$  and  $\text{Pb(NO}_3)_2$ . The abundances of  $\text{PbC}_2\text{O}_4$  and  $\text{Pb(NO}_3)_2$  in the size range > 10.2  $\mu\text{m}$  are very similar, whereas the abundance of  $2\text{PbCO}_3 \cdot \text{Pb(OH)}_2$  is slightly lower than for the aforementioned species. The most dominant species in the size ranges 10.2–4.2 and 4.2–2.1  $\mu\text{m}$  is  $2\text{PbCO}_3 \cdot \text{Pb(OH)}_2$ . For the fine aerosol particles,  $\text{PbC}_2\text{O}_4$  is the most dominant species in the range 2.1–1.3  $\mu\text{m}$  size fraction, whereas the dominant species in the range 1.3–0.69 and < 0.69  $\mu\text{m}$  size fractions is  $\text{Pb(NO}_3)_2$ . Thus, size fractionation of Pb species was found throughout the size ranges of the aerosol

Table 1 Abundances of Pb species for size-fractionated aerosol sample, Pb sources (%) and  $R$  values

	$2\text{PbCO}_3 \cdot \text{Pb(OH)}_2$	$\text{Pb(NO}_3)_2$	$\text{PbC}_2\text{O}_4$	$\text{PbCl}_2$	$\text{PbCO}_3$	$\text{PbSO}_4$	$\text{PbO}$	$R$ value
Single coarse aerosol	86	–	14	–	–	–	–	0.049
>10.2 $\mu\text{m}$	27	37	36	–	–	–	–	0.023
10.2–4.2 $\mu\text{m}$	54	12	34	–	–	–	–	0.022
4.2–2.1 $\mu\text{m}$	57	13	30	–	–	–	–	0.014
Single fine aerosol	–	29	71	–	–	–	–	0.033
2.1–1.3 $\mu\text{m}$	–	31	40	–	–	29	–	0.013
1.3–0.69 $\mu\text{m}$	–	44	31	–	–	25	–	0.017
< 0.69 $\mu\text{m}$	–	40	33	–	–	27	–	0.020
Resuspended particle	89	–	11	–	–	–	–	0.025
Road dust	89	–	11	–	–	–	–	0.028
Hiroshima granite	15	30	–	55	–	–	–	0.021
Fly ash (heavy oil)	–	33	27	–	40	–	–	0.021
Fly ash (MSWI)	–	20	27	–	–	53	–	0.015
Residual ash (MSWI)	–	–	–	31	–	–	69	0.021

\*  $R$  value is defined in Eq. (1) in the text.



particles examined. These findings clearly show that size fractionated analysis for chemical speciation of aerosol samples provides valuable new information on sources of Pb in the atmosphere and, in addition, give new insights into the formation mechanisms of aerosol particles.

Lead species in road dust and in resuspended particles were  $\text{PbC}_2\text{O}_4$  and  $2\text{PbCO}_3\cdot\text{Pb}(\text{OH})_2$ . The natural sample, the Hiroshima granite, contained  $\text{PbCl}_2$ ,  $2\text{PbCO}_3\cdot\text{Pb}(\text{OH})_2$ , and  $\text{Pb}(\text{NO}_3)_2$ . The XANES spectrum of Hiroshima granite is very flat and this feature is indicative of the presence of  $\text{PbCl}_2$ . Lead species in fly ash derived from MSWI and heavy oil combustion were  $\text{PbC}_2\text{O}_4\cdot\text{PbSO}_4\cdot\text{Pb}(\text{NO}_3)_2$  and  $\text{PbC}_2\text{O}_4\cdot\text{PbCO}_3\cdot\text{Pb}(\text{NO}_3)_2$ , respectively. These samples also contained  $\text{PbSO}_4$  and  $\text{Pb}(\text{NO}_3)_2$ . Therefore, the first peak tops are located at just less than 13.03 keV. Interestingly, the XANES spectra of fly ash and residual ash from MSWI were different. The spectrum of residual ash was quite characteristic because this spectrum reflects the presence of PbO which has peak top at the highest energy, 13.04 keV, amongst the reference materials used in this study. The lead species,  $\text{PbC}_2\text{O}_4$ ,  $\text{PbSO}_4$ , and  $\text{Pb}(\text{NO}_3)_2$ , were observed for fly ash collected immediately at the chimney exit, whereas  $\text{PbCl}_2$  and PbO were noted to be present in the residual ash. This result clearly showed that the formation of a particular Pb species may depend on the boiling points of each Pb compound in accord with the combustion processes (Verhulst et al., 1995). Thus in the case of Pb species derived from a MSWI, the Pb species in fly ash may be used as a possible source indicator of Pb species in the atmosphere. As for samples collected from the road tunnel, which represent aerosols emitted by motor traffic, Pb could not be measured due to the very low concentrations in the sample. Thus, Pb originating from automobile exhausts can probably be ignored as a major source of Pb emissions in Japan at the present time.

## 2.2 Formation mechanism of Pb species

Possible formation mechanisms for Pb species are shown in Table 2. The representative Pb source for coarse aerosol particles is road dust because  $2\text{PbCO}_3\cdot\text{Pb}(\text{OH})_2$  is the most dominant Pb species. Actually, it has been reported that  $2\text{PbCO}_3\cdot\text{Pb}(\text{OH})_2$  was contained in road dust (Biggins and Harrison, 1980; Barrett et al., 2010), although this was not the most dominant species in their analyses. Especially in Japan, there are many white traffic signs containing  $2\text{PbCO}_3\cdot\text{Pb}(\text{OH})_2$  and/or  $\text{PbCO}_3$ , painted on roadways. These Pb species can be released by the actions of weathering and ablation and can, over time, accumulate in road dust. In addition,  $2\text{PbCO}_3\cdot\text{Pb}(\text{OH})_2$  is the ultimate product of weathering of road dust (Hem and Durum, 1973). Long-term weathering by wind and rain/snow can transform  $\text{PbCO}_3$  to  $2\text{PbCO}_3\cdot\text{Pb}(\text{OH})_2$  at the road surface. Another main Pb species in road dust is  $\text{PbC}_2\text{O}_4$ . Although we cannot explain precisely how  $\text{PbC}_2\text{O}_4$  is formed in road dust,  $\text{PbC}_2\text{O}_4$  is formed either by (1) reactions at particle surfaces (Mochida et al., 2003; Furukawa and Takahashi, 2011) and/or (2) by metabolic processes involving fungi in soil (Dutton and Evans, 1996). Resuspended particles can consist mainly of wind-blown road dust, because Pb species in both samples were found to be essentially the same.

Emission from incinerators and oil combustion are considered to be the main sources of gaseous Pb that distribute in the fine particle size range and where  $\text{PbC}_2\text{O}_4$ ,  $\text{PbSO}_4$ ,  $\text{Pb}(\text{NO}_3)_2$ , and  $\text{PbCO}_3$  are the dominant species.

It is considered that  $\text{PbC}_2\text{O}_4$  in fine aerosol particles is formed in the atmosphere as a secondary process. From the results of Moffet et al. (2008), Pb and Zn particles generated from combustion process co-exist with oxalate ions. Dicarboxylic acid in the atmosphere is formed by photochemical oxidation of gaseous organic carbon (Kawamura and Ikushima, 1993). Actually, the dominant Ca and Zn species in fine aerosol particles were the metal oxalates (Furukawa and Takahashi, 2011). In addition, it

**Table 2** Formation mechanisms and sources of Pb in coarse and fine aerosol particles

Aerosol size	Lead species	Formation mechanisms of Pb species in atmosphere	Pb source
Coarse aerosol particles	$2\text{PbCO}_3\cdot\text{Pb}(\text{OH})_2$	From road dust. This species is derived from traffic sign paint on road (white)	Road dust
	$\text{PbC}_2\text{O}_4$	From road dust originally provided by reaction at particles surfaces or by metabolisms of fungi	Road dust
	$\text{Pb}(\text{NO}_3)_2$	$2\text{PbCO}_3\cdot\text{Pb}(\text{OH})_2$ is altered by chemical reaction with gas-phase $\text{HNO}_3$	
Fine aerosol particles	$\text{PbSO}_4$	Chemical reaction with $\text{H}_2\text{SO}_4$ on pre-existing particle (in-cloud process)	Fly ash of MSWI and heavy oil
	$\text{PbC}_2\text{O}_4$	Complex formation in atmosphere with oxalate ions	Fly ash of MSWI and heavy oil
	$\text{Pb}(\text{NO}_3)_2$	Chemical reaction with $\text{HNO}_3$ on pre-existing particle (in-cloud process)	Fly ash of MSWI and heavy oil

was suggested that Cu and Pb, which are emitted from anthropogenic sources, have the potential to form metal-oxalate complexes because (1) the stability constants of oxalate with Ca, Cu, Pb, and Zn are high (Martell and Smith, 1977) and (2) the solubilities of these metal complexes are very low (David, 1994). Thus,  $\text{PbC}_2\text{O}_4$  is a plausible species in gaseous (fine) aerosol particles such as fly ash.

Sulfates in fine aerosol particles are also formed by chemical reactions in the atmosphere such as oxidation of  $\text{SO}_2$  by reaction with  $\text{OH}\cdot$ ,  $\text{H}_2\text{O}_2$ , and  $\text{O}_3$  followed by condensation or nucleation of  $\text{H}_2\text{SO}_4$  on pre-existing particles. For example, new particles are formed by reaction with ammonia. It can be considered that  $\text{H}_2\text{SO}_4$  can react with heavy metals in pre-existing particles. In addition, the concentrations of sulfates and oxalates showed a good correlation with each other; this is because sulfate and oxalate, in the particle size range of ca. 0.5–2.0  $\mu\text{m}$ , have been formed by similar processes such as the in-cloud processes (Yao et al., 2002). For these reasons,  $\text{PbSO}_4$  can be found in fine aerosol particles together with  $\text{PbC}_2\text{O}_4$ .

Nitric acid in fine aerosol particles plays a key role in producing  $\text{Pb}(\text{NO}_3)_2$  in the atmosphere. There are two processes for formation of nitrate in fine aerosol particles. The first process is the gas-phase reaction of  $\text{HNO}_3$  with ammonia to form particles of diameter 0.1–0.3  $\mu\text{m}$ . Another process is that  $\text{HNO}_3$  reacts with pre-existing fine aerosol particles to form particles of 0.5–0.7  $\mu\text{m}$  diameter (Wall et al., 1988). Lead nitrate in fine aerosol particles may be formed by the latter process, since the former process is not likely to occur for Pb due to the low volatility of Pb compounds under ambient conditions.

Li and Shao (2009a) analyzed more than 800 particles in brown haze from North China by transmission electron microscope (TEM)-EDX. Osán et al. (2010) also sampled fine aerosol particles in Hungary and Austria and measured major metal species such as Zn and Cu. These elements may behave nearly the same as Pb, since these elements are divalent and has similar boiling points. Actually, Cu and Zn have been found in secondary aerosol particles in the form of sulfates together with nitrates. Thus,  $\text{PbSO}_4$  and  $\text{Pb}(\text{NO}_3)_2$  can be formed ubiquitously in fine particles notwithstanding differences in sampling locations and seasonality.

### 2.3 Sources of Pb based on Pb speciation and elemental concentration

#### 2.3.1 Coarse aerosol particles

The Pb species in coarse aerosol particles ( $> 2.1 \mu\text{m}$ ) were  $\text{PbC}_2\text{O}_4$ ,  $2\text{PbCO}_3\cdot\text{Pb}(\text{OH})_2$ , and  $\text{Pb}(\text{NO}_3)_2$ . Speciation analysis indicated that the source of coarse particles was road dust which mainly contained  $\text{PbC}_2\text{O}_4$  and  $2\text{PbCO}_3\cdot\text{Pb}(\text{OH})_2$ . This assignment was also supported by the concentration data and enrichment factors (EFs) for Cu (EF = 15) and Sb (EF = 500), as shown in Fig. S2,

Supplement. In the roadside or tunnel atmosphere, the concentrations of Cu and Sb are very high due to brake ablation emissions (Adachi and Tainsho, 2004; Bukowiecki et al., 2009). Road dusts have also been reported to be enriched in Cu and Sb (Birmili et al., 2006). Therefore, it is concluded that one of the sources for Pb in coarse aerosol particles is road dust.

As for  $\text{Pb}(\text{NO}_3)_2$  which was not contained in road dust, a possible explanation for its presence in the coarse fraction is that it is formed as a result of chemical reactions in the atmosphere such as between soil particles in aerosol form and gas-phase  $\text{HNO}_3$ . It has been reported that  $\text{CaCO}_3$  in soil was altered to  $\text{Ca}(\text{NO}_3)_2$  due to chemical reaction with gas-phase  $\text{HNO}_3$  (e.g. Pakkanen, 1996; Zhuang et al., 1999; Li and Shao., 2009b). Similarly, it is possible that gas-phase  $\text{HNO}_3$  can react with  $2\text{PbCO}_3\cdot\text{Pb}(\text{OH})_2$  in road dust and/or coarse aerosol particles, in the same way as  $\text{CaCO}_3$  in the atmosphere was altered to  $\text{Ca}(\text{NO}_3)_2$ . As a result, the abundance of  $2\text{PbCO}_3\cdot\text{Pb}(\text{OH})_2$  in coarse aerosol particles were lower than that of road dust, thus  $\text{Pb}(\text{NO}_3)_2$  can exist in the coarse aerosol fraction. In addition, the abundance of  $2\text{PbCO}_3\cdot\text{Pb}(\text{OH})_2$  was increased with a corresponding decrease in  $\text{Pb}(\text{NO}_3)_2$ . This type of reaction may explain the formation mechanism of  $\text{Pb}(\text{NO}_3)_2$  in coarse aerosol particles. Similar reactions also occur with  $\text{H}_2\text{SO}_4$  in the atmosphere. However, the concentration of gas-phase  $\text{H}_2\text{SO}_4$  is very low in both clean and polluted environments (Weber et al., 1995), because almost all  $\text{H}_2\text{SO}_4$  exists as condensed particles (ten Brink, 1998). In addition, the reactivity of  $\text{SO}_2$  with the mineral dusts are less than those of  $\text{HNO}_3$  and  $\text{NO}_2$  (Ooki and Uematsu, 2005). Therefore, gas-phase  $\text{HNO}_3$  can react with coarse aerosol particles much more efficiently than gas-phase  $\text{H}_2\text{SO}_4$ . As a result,  $\text{Pb}(\text{NO}_3)_2$  can be preferentially formed in the coarse aerosol particles.

#### 2.3.2 Fine aerosol particles

Lead species in fine aerosol particles were judged to be  $\text{PbC}_2\text{O}_4$ ,  $\text{PbSO}_4$ , and  $\text{Pb}(\text{NO}_3)_2$ . Emissions from MSWI are likely to be the dominant source for fine aerosol particles because the Pb speciation is essentially the same for the fine aerosol fraction and particles from MSWI. Also the size distributions for Pb and Cd, which are emitted from MSWI are very similar (Fig. S2 in Supporting materials) (Sakata et al., 2000; Birmili et al., 2006). The abundance of  $\text{PbSO}_4$  in fine aerosol particles is lower than that of fly ash from the MSWI and this may be explained by a dilution effect from another source such as ash from heavy oil combustion. Nickel and V, which are used as tracers for heavy oil (fuel) combustion have been shown to be concentrated in the finer aerosol particles (e.g. Nriagu and Pacyna, 1988; Wang et al., 2006; Mazzei et al., 2008). Our results also showed the presence of high concentration of Ni and V in finer aerosol particles (Fig. S2 in Supporting materials). Therefore, fly ash derived

from heavy oil combustion is one of the dominant Pb sources. However, Pb from heavy oil combustion is not the dominant source of Pb in the fine fraction because the abundance of  $\text{PbCO}_3$  in fly ash from oil combustion was not a major component in the fine aerosol particles. Therefore, it can be concluded that MSWI is one of the dominant Pb sources in fine aerosol particles, followed by fly ash from heavy oil combustion. Lead species in all environmental samples and sources of emission are shown in Table 2.

The reliability of Pb speciation in the aerosol sample was confirmed by  $\mu$ -XRF-XAFS analysis of individual aerosol particles. The results showed that Pb species in single aerosol particles were very similar to those from bulk XAFS analysis (Sakata et al., in prep.). Furthermore, the formation mechanisms of all Pb species in both coarse and fine aerosol particles can be explained by similar reactions of major components (Na, Ca, and  $\text{NH}_3$ ) and physical behavior such as resuspension of road dust. Thus, the results obtained in this study are considered robust and reliable for chemical speciation of Pb in aerosols and for the formation mechanisms of aerosols in the atmosphere.

In this study, we have examined only one sample which was obtained in the autumn, a season without remarkable climatic events. This limited sampling and analysis is clearly not sufficient to permit a rigorous assessment of formation mechanisms of Pb species in aerosol particles throughout the year. However, we believe that our findings may be one of the key first steps to discuss the formation mechanisms of aerosols and the reaction of metallic elements in the atmosphere.

It is considered that Pb species in the atmosphere can be used as a tool to identify Pb sources because Pb species in atmospheric aerosol retain the characteristic Pb species fingerprint of each source. In addition, Pb species in the atmosphere are different between Higashi-Hiroshima and other locations such as Osaka and Beijing due to the differences in Pb source emissions (Tan et al., 2006; Funasaka et al., 2008). Therefore, there is a possibility that Pb species in the atmosphere may serve as tracers of local emission sources. Furthermore, it is suggested that Pb in the atmosphere cannot be considered as a health hazard based on the Pb concentrations revealed in this work. The total Pb concentration in Higashi-Hiroshima was about  $20 \text{ ng/m}^3$  (Supporting materials) which is much lower than the health criterion standard set for Pb in the atmosphere ( $150 \text{ ng/m}^3$ ). However, ongoing environmental reconnaissance is needed given that atmospheric Pb is concentrated in  $\text{PM}_{2.5}$  which, on inhalation, can penetrate into the lung.

### 3 Conclusions

In this study, Pb species, size-distributions of major ions, and heavy metal concentrations at Higashi-Hiroshima

were determined by XANES spectroscopy, ion chromatography, and ICP-MS/AES, respectively. The total Pb concentration in the sampled air was about  $20 \text{ ng/m}^3$  and about 80% of total Pb was concentrated in the fine aerosol particles. The total Pb concentration was much lower than  $150 \text{ ng/m}^3$ , the health criterion standard for atmospheric Pb. Lead speciation for all size fractions was successfully clarified by the Pb L<sub>III</sub>-edge XANES measurement which employed a double-crystal of Si(311) for enhanced energy resolution. In addition,  $\mu$ -XRF-XAFS analysis were also conducted for the confirmation of accuracy of the combination of Pb species in each size fractionated particle. Lead species were different for the fine and coarse aerosol size fractions. The Pb species in the coarse aerosol particles were  $\text{PbC}_2\text{O}_4$ ,  $2\text{PbCO}_3\cdot\text{Pb}(\text{OH})_2$ , and  $\text{Pb}(\text{NO}_3)_2$  and the main source of Pb was road dust because the main Pb components in road dust were  $\text{PbC}_2\text{O}_4$  and  $2\text{PbCO}_3\cdot\text{Pb}(\text{OH})_2$ . Source appropriation was also suggested by the EFs for Cu and Sb which are good source indicators of road dust. Lead nitrate in coarse aerosol particles, which was not contained in road dust, might be formed by atmospheric chemical reaction of  $2\text{PbCO}_3\cdot\text{Pb}(\text{OH})_2$  with gas-phase  $\text{HNO}_3$ . In contrast, the Pb species in fine aerosol particles were  $\text{PbC}_2\text{O}_4$ ,  $\text{PbSO}_4$ , and  $\text{Pb}(\text{NO}_3)_2$  and the major Pb sources were fly ash derived from MSWI and heavy oil combustion, based on the characterization of Pb species in these source materials. This result was also supported by size-distribution measurements of Cd, Ni, and V. Thus, Pb species in atmospheric aerosol can be a good indicator of sources of Pb emission.

Thus, sources of Pb in fine and coarse aerosol particles can be established through Pb speciation measurement together with the determination of major and trace element concentrations. These results may serve as guidelines to avoid health effects from Pb exposure. Furthermore, the speciation results serve as an aid for using Pb as a tracer of air-mass transportation/circulation following the abolition of leaded gasoline.

### Acknowledgments

We thank office staff in Kamo Environmental Health Center for help in sampling. This study was performed with the approval of KEK-PF (2011G644 and 2012G111) and SPring-8 (2012A1299, 2012B1428, and 2012B1564).

### Supporting materials

Supplementary data associated with this article can be found in the online version.

### REFERENCES

- Adachi, K., Tainsho, Y., 2004. Characterization of heavy metal particles embedded in tire dust. *Environ. Int.* 30, 1009–1017.
- Barrett, J.E.S., Taylor, K.G., Edwards, K.A.H., Charnock, J.M., 2010.

- Solid-phase speciation of Pb in urban road dust sediment: A XANES and EXAFS study. *Environ. Sci. Technol.* 44, 2940–2946.
- Biggins, P.D.E., Harrison, R.M., 1979. Atmospheric chemistry of automotive lead. *Environ. Sci. Technol.* 13, 558–565.
- Biggins, P.D.E., Harrison, R.M., 1980. Chemical speciation of lead compounds in street dusts. *Environ. Sci. Technol.* 14, 337–339.
- Birmili, W., Allen, A.G., Bary, F., Harrison, R.M., 2006. Trace metal concentrations and water solubility in size-fractionated atmospheric particles and influence of road traffic. *Environ. Sci. Technol.* 40, 1144–1153.
- Bollhöfer, A., Rosman, K.J.R., 2000. Isotopic source signatures for atmospheric lead: The Southern Hemisphere. *Geochim. Cosmochim. Acta* 64, 3251–3262.
- Bollhöfer, A., Rosman, K.J.R., 2001. Isotopic source signatures for atmospheric lead: The Northern Hemisphere. *Geochim. Cosmochim. Acta* 65, 1727–1740.
- Bukowiecki, N., Lienemann, P., Hill, M., Figi, R., Richard, A., Furger, M. et al., 2009. Real-world emission factors for antimony and other brake wear related trace elements: Size-segregated values for light and heavy duty vehicles. *Environ. Sci. Technol.* 43, 8072–8078.
- Chen, J., Tan, M., Li, Y., Zhang, Y., Lu, W., Tong, Y. et al., 2005. A lead isotope record of shanghai atmospheric lead emissions in total suspended particles during the period of phasing out of leaded gasoline. *Atmos. Environ.* 39, 1245–1253.
- David, R., 1994. *Handbook of Chemistry and Physics*, 75th ed. CRC Press Inc., USA.
- Dutton, M.V., Evans, C.S., 1996. Oxalate production by fungi: its role in pathogenicity and ecology in the soil environment. *Can. J. Microbiol.* 42, 881–895.
- Funasaka, K., Tojo, T., Katahira, K., Shinya, M., Miyazaki, T., Kamiura, T. et al., 2008. Detection of Pb-LIII edge XANES spectra of urban atmospheric particles combined with simple acid extraction. *Sci. Total Environ.* 403, 230–234.
- Furukawa, T., Takahashi, Y., 2011. Oxalate metal complexes in aerosol particles: implication for the hygroscopicity of oxalate-containing particles. *Atmos. Chem. Phys.* 11, 4289–4301.
- Hem, J.D., Durum, W.H., 1973. Solubility and occurrence of lead in surface water. *J. Am. Water Works Assoc.* 65: 562–568.
- Higashi, M., Takahashi, Y., 2009. Detection of S(IV) species in aerosol particles using XANES spectroscopy. *Environ. Sci. Technol.* 43, 7357–7363.
- Inoue, M., Tanimizu, M., 2008. Anthropogenic lead inputs to the western Pacific during the 20th century. *Sci. Total Environ.* 405, 123–130.
- Jacob, D.J., 1999. *Introduction to Atmospheric Chemistry*. Princeton University Press, New Jersey, USA.
- Kawamura, K., Ikushima, K., 1993. Seasonal changes in the distribution of dicarboxylic acids in the urban atmosphere. *Environ. Sci. Technol.* 27, 2227–2235.
- Li, W.J., Shao, L.Y., 2009a. Transmission electron microscopy study of aerosol particles from the brown hazes in northern China. *J. Geophys. Res.* 114. DOI: 10.1029/2008JD011285.
- Li, W.J., Shao, L.Y., 2009b. Observation of nitrate coatings on atmospheric mineral dust particles. *Atmos. Chem. Phys.* 9, 1894–1871.
- Linton, R.W., Natusch, D.F.S., Solomon, R.L., Evans, Jr., C.A., 1980. Physicochemical characterization of lead in urban dusts. A Microanalytical approach to lead tracing. *Environ. Sci. Technol.* 14, 159–164.
- Manceau, A., Boisset, M.C., Sarret, G., Hazemann, J.L., Mench, M., Cambier, P. et al., 1996. Direct determination of lead speciation in contaminated soils by EXAFS spectroscopy. *Environ. Sci. Technol.* 30, 1540–1552.
- Maring, H., Settle, D.M., Ménard, P.B., Dulac, F., Patterson, C.C., 1987. Stable lead isotope tracers of air mass trajectories in the Mediterranean region. *Nature* 330, 154–156.
- Martell, A.E., Smith, R.M., 1977. *Critical Stability Constants*, volume-3, Other Organic Ligands, Plenum, New York, USA.
- Mazzei, F., D'Alessandro, A., Lucarelli, F., Nava, S., Prati, P., Valli, G. et al., 2008. Characterization of particulate matter sources in an urban environment. *Sci. Total Environ.* 401, 81–89.
- Mizoguchi, T., Zhang, J., Satake, H., Mukai, H., Murano, K., Kawasaki, K., 2012. Lead and sulfur isotopic ratios in precipitation and their relations to trans-boundary atmospheric pollution. *Atmos. Res.* 104, 237–244.
- Mochida, M., Kawamura, K., Uemoto, N., Kobayashi, M., Matsunaga, S., Lim, H.J. et al., 2003. Spatial distributions of oxygenated organic compounds (dicarboxylic acids, fatty acids, and levoglucosan) in marine aerosol over the western Pacific and off the coast of East Asia: Continental outflow of organic aerosols during the ACE-Asia campaign. *J. Geophys. Res.* 108, 8638. DOI: 10.1029/2002JD003249.
- Moffet, R.C., Desyaterik, Y., Hopkins, R.J., Tivanski, A.V., Gilles, M.K., Wang, Y. et al., 2008. Characterization of aerosols containing Zn, Pb, and Cl from an industrial region of Mexico city. *Environ. Sci. Technol.* 42, 7091–7097.
- Mukai, H., Furuta, N., Fujii, T., Ambe, Y., Sakamoto, K., Hashimoto, Y., 1993. Characterization of sources of lead in the urban air of Asia using ratios of stable lead isotopes. *Environ. Sci. Technol.* 27, 1347–1356.
- Mukai, H., Tanaka, A., Fujii, T., Nakao, M., 1994. Lead isotope ratios of airborne particulate matter as tracers of long-range transport of air pollutants around Japan. *J. Geophys. Res.* 99, 3717–3726.
- Murphy, D.M., Hudson, P.K., Cziczko, D.J., Gallavardin, S., Froyd, K. D., Johnston, M.V. et al., 2007. Distribution of lead in single atmospheric particles. *Atmos. Chem. Phys.* 7, 3195–3210.
- Nriagu, J.O., 1990. The rise and fall of leaded gasoline. *Sci. Total Environ.* 92, 13–28.
- Nriagu, J.O., Pacyna, J.M., 1988. Quantitative assessment of worldwide contamination of air, water and soils by trace metals. *Nature* 333, 134–139.
- Ooki, A., Uematsu, M., 2005. Chemical interactions between mineral dust particles and acid gases during Asian dust events. *J. Geophys. Res.* 110. DOI: 10.1029/2004JD004737.
- Osán, J., Meirer, F., Groma, V., Török, S., Ingerle, D., Strelí, C. et al., 2010. Speciation of copper and zinc in size-fractionated atmospheric particulate matter using total reflection mode X-ray absorption near-edge structure spectrometry. *Spectrochimica Acta, Part B: Atomic Spectrosc.* 65, 1008–1013.
- Pakkanen, T.A., 1996. Study of formation of coarse particle nitrate aerosol. *Atmos. Environ.* 30, 2475–2482.
- Rabinowitz, M.B., Wetherill, G.W., 1972. Identifying sources of lead contamination by stable isotope techniques. *Environ. Sci. Technol.* 6, 705–709.
- Sakata, M., Kurata, M., Tanaka, N., 2000. Estimation contribution from municipal solid waste incineration to trace metal concentrations in Japanese urban atmosphere using lead as a marker element. *Geochem. J.* 34, 23–32.

- Sakata, K., Sakaguchi, A., Tanimizu, M., Yokoyama, Y., Takahashi, Y., in prep. Lead speciation analyses of coarse and fine aerosol particles by bulk and micro X-ray absorption fine structure spectroscopy.
- Salma, I., Maenhaut, W., Záray, G., 2002. Comparative study of elemental mass size distribution in urban atmospheric aerosol. *J. Aerosol Sci.* 33, 339–356.
- Shimamura, T., Iijima, S., Iwashita, M., Hattori, M., Takaku, Y., 2007. Lead isotope in rainfall collected by a sequential sampler in suburban Tokyo. *Atmos. Environ.* 41, 3797–3805.
- Sturges, W. T., Harrison, R. M., 1989. Semi-quantitative X-ray diffraction analysis of size fractionated atmospheric particles. *Atmos. Environ.* 23, 1083–1098.
- Takahashi, Y., Kanai, Y., Kamioka, H., Ohta, A., Maruyama, H., Song, Z. et al., 2006. Speciation of sulfate in size-fractionated aerosol particles using sulfur K-edge X-ray absorption near-edge structure (XANES). *Environ. Sci. Technol.* 40, 5052–5057.
- Tan, M.G., Zhang, G.L., Li, X.L., Zhang, Y.X., Yue, W.S., Chen, J.M. et al., 2006. Comprehensive study of lead pollution in shang hai by multiple techniques. *Anal. Chem.* 78, 8044–8050.
- ten Brink, H.M., 1998. Reactive uptake of  $\text{HNO}_3$  and  $\text{H}_2\text{SO}_4$  in sea-salt (NaCl) particles. *J. Aerosol. Sci.* 29, 57–64.
- Terada, Y., Goto, S., Takimoto, N., Takeshita, K., Yamazaki, H., Shimizu, Y., Takahashi, S. et al., 2004. Construction and commissioning of BL37XU at SPring-8. *AIP Conference Proc.* 705, 376–379.
- Verhulst, D., Buekens, A., Spencer, P.J., Eriksson, G., 1995. Thermodynamic behavior of metal chlorides and sulfates under the conditions of incinerator furnaces. *Environ. Sci. Technol.* 30, 50–56.
- Wall, S.M., Johnston, W., Ondo, J.L., 1988. Measurement of aerosol size distributions for nitrate and major ionic species. *Atmos. Environ.* (1967) 22, 1649–1656.
- Wang, X., Sato, T., Xing, B., 2006. Size distribution and anthropogenic sources apportionment of airborne trace metals in Kanazawa, Japan. *Chemosphere* 65, 2440–2448.
- Wang, X., Sato, T., Xing, B., Tamamura, S., Tao, S., 2005. Source identification, size distribution and indicator screening of airborne trace metals in Kanazawa, Japan. *J. Aerosol Sci.* 36, 197–210.
- Weber, R. J., McMurry, P.H., Eisele, F.L., Tanner, D.J., 1995. Measurement of expected nucleation precursor species and 3-500-nm diameter particles at Mauna Loa observatory, Hawaii. *J. Atmos. Sci.* 52, 2242–2257.
- Yao, X., Fang, M., Chan, C.K., 2002. Size distributions and formation of dicarboxylic acids in atmospheric particles. *Atmos. Environ.* 36, 2099–2107.
- Yao, X., Lau, A.P.S., Fang, M., Chan, C. K., Hu, M., 2003. Size distributions and formation of ionic species in atmospheric particulate pollutants in Beijing, China: 2-dicarboxylic acids. *Atmos. Environ.* 37, 3001–3007.
- Zhuang, H., Chan, C.K., Fang, M., Wexler, A.S., 1999. Size distribution of particulate sulfate, nitrate, and ammonium at coastal site in Hong Kong. *Atmos. Environ.* 33, 843–853.



## Supplement

### 1. Determination of major ion concentrations

Major ions concentrations were measured using the procedure of Furukawa and Takahashi (2011). A piece of filter paper was soaked in a 7 mL PFA Teflon vial containing 0.2 mL of ethanol and 5 mL of 18.2 MΩ MQ water. Ultrasonic treatment was carried out for 30 minutes to extract major ions. These solutions were filtered with a 0.20 μm hydrophilic PTFE filter (DISMIC®-25, ADVANTEC, Japan). Measurement of cations ( $\text{Na}^+$ ,  $\text{NH}_4^+$ ,  $\text{K}^+$ ,  $\text{Ca}^{2+}$ , and  $\text{Mg}^{2+}$ ) and anions ( $\text{F}^-$ ,  $\text{Cl}^-$ ,  $\text{NO}_2^-$ ,  $\text{NO}_3^-$ ,  $\text{PO}_4^{3-}$ , and  $\text{SO}_4^{2-}$ ) was performed by ion chromatography (ICS-1100, Dionex, Japan), which consisted of separation columns (Dionex Ion Pac AS22 for anions and Ion Pac CS12A for cations) and guard columns (Dionex Ionpac AG22 for anions and IonPac CG12A for cations) in a thermo controlled oven (30°C). The eluent for anions was a mixed solution of 4.5 mmol/L  $\text{Na}_2\text{CO}_3$  and 1.4 mmol/L  $\text{NaHCO}_3$  and the eluent for cations was 20 mmol/L methanesulfonic acid. The flow rates of eluent for anion and cation measurement were fixed at 1.0 mL/min and 1.2 mL/min, respectively. The run time for each sample was 15 min.

Major ion concentrations are indicators for Pb sources and chemical reactions in the atmosphere. **Figure S1** shows major ion concentrations for all size fractions of aerosols studied. These results show that we can divide major cations into two distinct groups based on size-distribution. The first group has a unimodal pattern distribution whose peak corresponds to that of coarse aerosol particles. Sodium ion,  $\text{Ca}^{2+}$ , and  $\text{Mg}^{2+}$  belong to this category. The concentration ranges for  $\text{Na}^+$ ,  $\text{Ca}^{2+}$ , and  $\text{Mg}^{2+}$  were, 5.6 to 525 ng/m<sup>3</sup>, 31.4 to 118 ng/m<sup>3</sup>, and 4.59 to 68.4 ng/m<sup>3</sup>, respectively. The other distribution type is also unimodal but the peak corresponds to fine aerosol particles. Potassium and ammonium ions are in this second group. The concentrations ranges for  $\text{K}^+$  and ammonium ion are 8.81 to 83.6 ng/m<sup>3</sup> and 19.9 to 1303 ng/m<sup>3</sup>, respectively. As for the counter anions, fluoride, nitrite and phosphate, concentrations were below the limits of detection (fluoride: 30 ppb nitrite: 500 ppb

phosphate: 300 ppb). The concentrations of chloride, nitrate, and sulfate were in the range 98.1--641, 211--936, and 75.5--2575 ng/m<sup>3</sup>, respectively. Chloride and nitrate ions tended to concentrate in the coarse aerosol particles, whereas sulfate ion was more prevalent in the fine aerosol fraction. The size-distributions for these ions were comparable to previous studies (e.g. Kerminen et al., 1997)

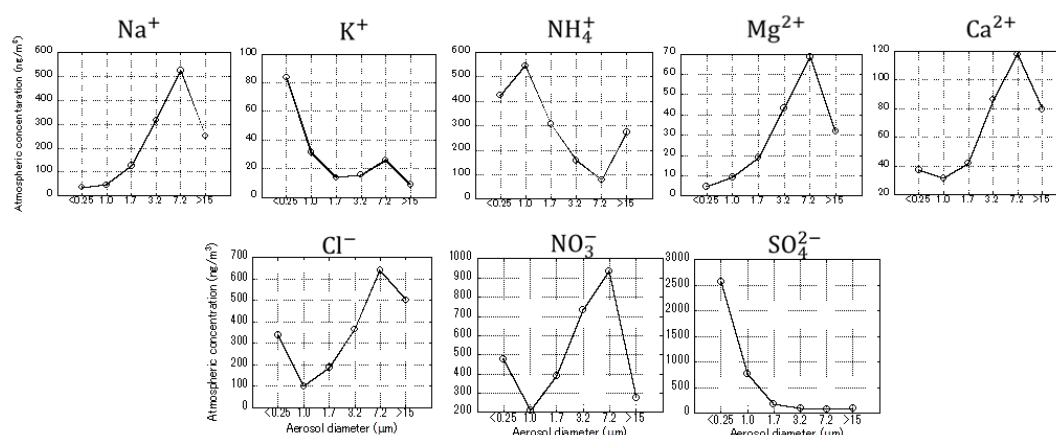


Fig. S1 Size distributions of atmospheric concentrations for major ions

## 2. Determination of trace metals concentrations

All sample filters were cut into appropriate size for analysis. In this case, to achieve representative and comparable results with XAFS analysis, the samples used were more than 10 (10--2000) times greater than that of the measurable volume for the target elements. The filter paper pieces were weighed into 7 mL PFA Teflon vials. All the samples were decomposed by heating with mixed mineral acid (2 mL of 15 mol/L HNO<sub>3</sub>, 2 mL of 6 mol/L HCl, and 1 mL of 20 mol/L HF) on a hot plate (90°C) for 12 hr. After decomposition, the solutions were evaporated to dryness. Then, each sample was redissolved in 4 mL of 0.15 mol/L HNO<sub>3</sub> and sample solutions heated at 90°C for 3 hr. Sample solutions were diluted to the appropriate concentration with 0.15 mol/L HNO<sub>3</sub>. Sample digests were analyzed for Al, Ba, Cd, Co, Cr, Cu, Fe, Mn, Ni, Pb, Sb, Sr, Ti, V, and Zn and concentrations, except for Fe, were determined by inductively-coupled plasma mass spectrometry (ICP-MS: Agilent 7700, Agilent Technologies, Japan). Iron was determined by ICP atomic emission

spectroscopy (ICP-AES: SPS-3500, SII Nano Technology, Japan). Indium was used as an internal standard for ICP-MS measurement.

The size-distribution and ratios of heavy metal concentrations such as Ni and V are good indicators of emission sources (e.g. Wang et al., 2006; Mazzei et al., 2008). **Figure S2** shows the size-distribution of atmospheric concentrations for 15 heavy metals. Lead concentration ranged from 0.80--8.4 ng/m<sup>3</sup>, and the total Pb concentration was estimated to be about 20 ng/m<sup>3</sup> in Higashi-Hiroshima. Compared to other cities in Japan such as Kanazawa and Tokyo, the Pb concentration in Higashi-Hiroshima was about four times higher than that of Kanazawa (Wang et al., 2005) and lower than that of Tokyo (Sakata et al., 2000). There are many Pb sources in major urban centers, whereas there will be much fewer sources for suburban areas like Higashi-Hiroshima and Kanazawa. Thus, the highest Pb concentration occurs in Tokyo, followed by Higashi-Hiroshima and Kanazawa. The Pb concentration in Tokyo, however, is much lower than the criterion concentration for Pb (0.15 µg/m<sup>3</sup>) in the atmosphere (NAAQS, EPA).

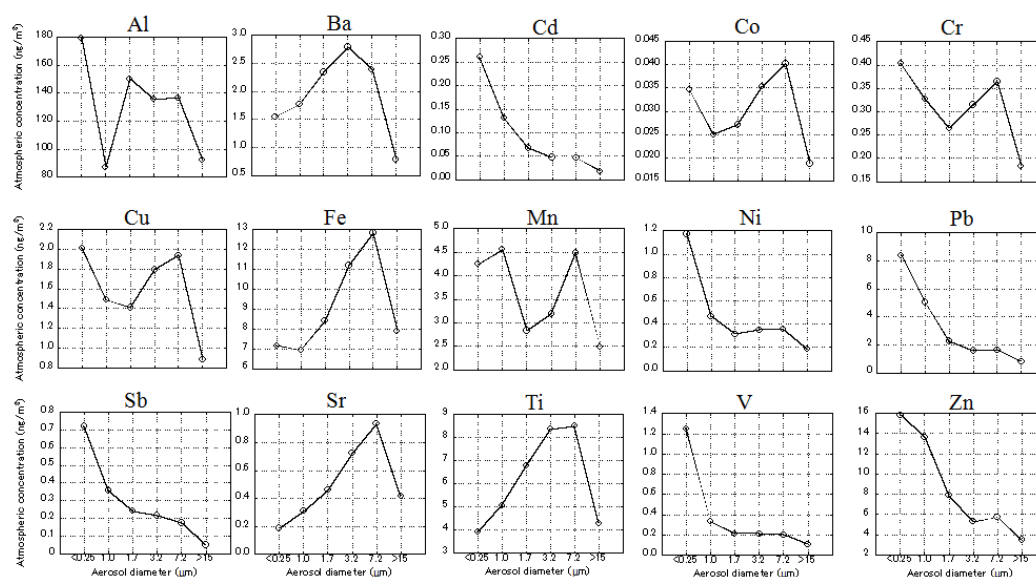


Fig. S2 Size distributions of atmospheric concentrations for heavy metals.

About 80% of total atmospheric Pb was found to be concentrated in the fine size fraction. Cadmium, Ni, V, Sb, and Zn had similar size-distributions to Pb and all had

high enrichment factors ( $EFs = \frac{X_{\text{sample}}/Al_{\text{sample}}}{X_{\text{crust}}/Al_{\text{crust}}}$ ) compared with the crustal abundance (e.g. EF of Pb is 92 to 606). As mentioned in main body text, almost all fine aerosol particles ( $< 2.1 \mu\text{m}$ ) are formed by condensation processes from precursor gases (Jacob, 1999). The aforementioned elements tend to be derived from anthropogenic gaseous emission sources. Barium, Fe, Sr, and Ti were concentrated in the coarse size fraction and exhibited the same unimodal distribution as Na, Mg, and Ca. The dominant sources for these elements were from natural sources because the EFs of these elements (Na, Mg, and Ca) were below 10. Size-distributions for Al, Co, Cu, Cr, and Mn showed bimodal peaks both in the fine and coarse particle size ranges. The EFs for Al, Co, Cr, and Mn were below 10 for all particle size fractions, suggesting that these elements were derived from natural sources. On the other hand, the EF of Cu was greater than 10 for all size fractions which implies that Cu was of anthropogenic origin. The size-distributions of almost all trace metals measured in this study were comparable to those obtained in Kanazawa (Wang et al., 2006). These authors concluded that key anthropogenic elements such as Cd, Pb, V, and Zn in Kanazawa were derived from oil combustion and MSWI. Therefore, it is similarly judged that the major source of these elements in Higashi-Hiroshima is the same as in Kanazawa.

#### Reference

- Kerminen, V. M., Pakkanen, T. A., Hillamo, R. E., 1997. Interactions between inorganic trace gases and supramicrometer particles at a coastal site. *Atmos. Environ.* 31: 2753--2765.



## Editorial Board of Journal of Environmental Sciences

### Editor-in-Chief

**Hongxiao Tang** Research Center for Eco-Environmental Sciences, Chinese Academy of Sciences, China

### Associate Editors-in-Chief

**Jiuhui Qu** Research Center for Eco-Environmental Sciences, Chinese Academy of Sciences, China  
**Shu Tao** Peking University, China  
**Nigel Bell** Imperial College London, United Kingdom  
**Po-Keung Wong** The Chinese University of Hong Kong, Hong Kong, China

### Editorial Board

#### Aquatic environment

**Baoyu Gao**  
Shandong University, China  
**Maohong Fan**  
University of Wyoming, USA  
**Chihpin Huang**  
National Chiao Tung University  
Taiwan, China  
**Ng Wun Jern**  
Nanyang Environment &  
Water Research Institute, Singapore  
**Clark C. K. Liu**  
University of Hawaii at Manoa, USA  
**Hokyoung Shon**  
University of Technology, Sydney, Australia  
**Zijian Wang**  
Research Center for Eco-Environmental Sciences,  
Chinese Academy of Sciences, China  
**Zhiwu Wang**  
The Ohio State University, USA  
**Yuxiang Wang**  
Queen's University, Canada  
**Min Yang**  
Research Center for Eco-Environmental Sciences,  
Chinese Academy of Sciences, China  
**Zhifeng Yang**  
Beijing Normal University, China  
**Han-Qing Yu**  
University of Science & Technology of China

#### Terrestrial environment

**Christopher Anderson**  
Massey University, New Zealand  
**Zucong Cai**  
Nanjing Normal University, China  
**Xinbin Feng**  
Institute of Geochemistry,  
Chinese Academy of Sciences, China  
**Hongqing Hu**  
Huazhong Agricultural University, China  
**Kin-Che Lam**  
The Chinese University of Hong Kong  
Hong Kong, China  
**Erwin Klumpp**  
Research Centre Juelich, Agrosphere Institute  
Germany  
**Peijun Li**  
Institute of Applied Ecology,  
Chinese Academy of Sciences, China

#### Michael Schloter

German Research Center for Environmental Health  
Germany  
**Xuejun Wang**  
Peking University, China  
**Lizhong Zhu**  
Zhejiang University, China

#### Atmospheric environment

**Jianmin Chen**  
Fudan University, China  
**Abdelwahid Mellouki**  
Centre National de la Recherche Scientifique  
France  
**Yujing Mu**  
Research Center for Eco-Environmental Sciences,  
Chinese Academy of Sciences, China  
**Min Shao**  
Peking University, China  
**James Jay Schauer**  
University of Wisconsin-Madison, USA  
**Yuesi Wang**  
Institute of Atmospheric Physics,  
Chinese Academy of Sciences, China  
**Xin Yang**  
University of Cambridge, UK

#### Environmental biology

**Yong Cai**  
Florida International University, USA  
**Henner Hollert**  
RWTH Aachen University, Germany  
**Jae-Seong Lee**  
Hanyang University, South Korea  
**Christopher Rensing**  
University of Copenhagen, Denmark  
**Bojan Sedmak**  
National Institute of Biology, Ljubljana  
**Lirong Song**  
Institute of Hydrobiology,  
the Chinese Academy of Sciences, China  
**Chunxia Wang**  
National Natural Science Foundation of China  
**Gehong Wei**  
Northwest A & F University, China  
**Daqiang Yin**  
Tongji University, China  
**Zhongtang Yu**  
The Ohio State University, USA

#### Environmental toxicology and health

**Jingwen Chen**  
Dalian University of Technology, China  
**Jianying Hu**  
Peking University, China  
**Guibin Jiang**  
Research Center for Eco-Environmental Sciences,  
Chinese Academy of Sciences, China  
**Sijin Liu**  
Research Center for Eco-Environmental Sciences,  
Chinese Academy of Sciences, China  
**Tsuyoshi Nakanishi**  
Gifu Pharmaceutical University, Japan  
**Willie Peijnenburg**  
University of Leiden, The Netherlands  
**Bingsheng Zhou**  
Institute of Hydrobiology,  
Chinese Academy of Sciences, China

#### Environmental catalysis and materials

**Hong He**  
Research Center for Eco-Environmental Sciences,  
Chinese Academy of Sciences, China  
**Junhua Li**  
Tsinghua University, China  
**Wenfeng Shangguan**  
Shanghai Jiao Tong University, China  
**Yasutake Teraoka**  
Kyushu University, Japan  
**Ralph T. Yang**  
University of Michigan, USA

#### Environmental analysis and method

**Zongwei Cai**  
Hong Kong Baptist University,  
Hong Kong, China  
**Jiping Chen**  
Dalian Institute of Chemical Physics,  
Chinese Academy of Sciences, China  
**Minghui Zheng**  
Research Center for Eco-Environmental Sciences,  
Chinese Academy of Sciences, China

#### Municipal solid waste and green chemistry

**Pinjing He**  
Tongji University, China  
**Environmental ecology**  
**Rusong Wang**  
Research Center for Eco-Environmental Sciences,  
Chinese Academy of Sciences, China

### Editorial office staff

**Managing editor** Qingcai Feng  
**Editors** Zixuan Wang Suqin Liu Zhengang Mao  
**English editor** Catherine Rice (USA)



# JOURNAL OF ENVIRONMENTAL SCIENCES

环境科学学报(英文版)  
(<http://www.jesc.ac.cn>)

## Aims and scope

*Journal of Environmental Sciences* is an international academic journal supervised by Research Center for Eco-Environmental Sciences, Chinese Academy of Sciences. The journal publishes original, peer-reviewed innovative research and valuable findings in environmental sciences. The types of articles published are research article, critical review, rapid communications, and special issues.

The scope of the journal embraces the treatment processes for natural groundwater, municipal, agricultural and industrial water and wastewaters; physical and chemical methods for limitation of pollutants emission into the atmospheric environment; chemical and biological and phytoremediation of contaminated soil; fate and transport of pollutants in environments; toxicological effects of terrorist chemical release on the natural environment and human health; development of environmental catalysts and materials.

## For subscription to electronic edition

Elsevier is responsible for subscription of the journal. Please subscribe to the journal via <http://www.elsevier.com/locate/jes>.

## For subscription to print edition

China: Please contact the customer service, Science Press, 16 Donghuangchenggen North Street, Beijing 100717, China. Tel: +86-10-64017032; E-mail: [journal@mail.sciencep.com](mailto:journal@mail.sciencep.com), or the local post office throughout China (domestic postcode: 2-580).

Outside China: Please order the journal from the Elsevier Customer Service Department at the Regional Sales Office nearest you.

## Submission declaration

Submission of an article implies that the work described has not been published previously (except in the form of an abstract or as part of a published lecture or academic thesis), that it is not under consideration for publication elsewhere. The submission should be approved by all authors and tacitly or explicitly by the responsible authorities where the work was carried out. If the manuscript accepted, it will not be published elsewhere in the same form, in English or in any other language, including electronically without the written consent of the copyright-holder.

## Submission declaration

Submission of the work described has not been published previously (except in the form of an abstract or as part of a published lecture or academic thesis), that it is not under consideration for publication elsewhere. The publication should be approved by all authors and tacitly or explicitly by the responsible authorities where the work was carried out. If the manuscript accepted, it will not be published elsewhere in the same form, in English or in any other language, including electronically without the written consent of the copyright-holder.

## Editorial

Authors should submit manuscript online at <http://www.jesc.ac.cn>. In case of queries, please contact editorial office, Tel: +86-10-62920553, E-mail: [jesc@263.net](mailto:jesc@263.net), [jesc@rcees.ac.cn](mailto:jesc@rcees.ac.cn). Instruction to authors is available at <http://www.jesc.ac.cn>.

## Journal of Environmental Sciences (Established in 1989)

Vol. 26 No. 2 2014

<b>Supervised by</b>	Chinese Academy of Sciences	<b>Published by</b>	Science Press, Beijing, China
<b>Sponsored by</b>	Research Center for Eco-Environmental Sciences, Chinese Academy of Sciences		Elsevier Limited, The Netherlands
<b>Edited by</b>	Editorial Office of Journal of Environmental Sciences P. O. Box 2871, Beijing 100085, China Tel: 86-10-62920553; <a href="http://www.jesc.ac.cn">http://www.jesc.ac.cn</a> E-mail: <a href="mailto:jesc@263.net">jesc@263.net</a> , <a href="mailto:jesc@rcees.ac.cn">jesc@rcees.ac.cn</a>	<b>Distributed by</b>	
		Domestic	Science Press, 16 Donghuangchenggen North Street, Beijing 100717, China Local Post Offices through China
		Foreign	Elsevier Limited <a href="http://www.elsevier.com/locate/jes">http://www.elsevier.com/locate/jes</a>
<b>Editor-in-chief</b>	Hongxiao Tang	<b>Printed by</b>	Beijing Beilin Printing House, 100083, China
CN 11-2629/X	Domestic postcode: 2-580		Domestic price per issue RMB ¥ 110.00

ISSN 1001-0742

